AIMS Energy, 14(1): 89–114.
DOI: 10.3934/energy.2026004
Received: 20 June 2025
Revised: 09 September 2025
Accepted: 18 November 2025
Published: 15 January 2026

https://www.aimspress.com/journal/energy

Research article

Valorization of waste cooking oil, plantain peel and snail shell for the optimization of biodiesel production

Vincent E. Efeovbokhan[1,*], Ubong E. Usoro[1], Omololu O. Fagbiele[2] and Olubunmi G. Abatan[1]

[1] Department of Chemical Engineering, Covenant University, Ota, Nigeria
[2] Heriot-Watt University, School of Engineering and Physical Sciences, Scotland, UK

*** Correspondence:** Email: vincent.efeovbokhan@covenantuniversity.edu.ng; Tel: +2348052023977.

Abstract: Biodiesel is a viable alternative to non-renewable fossil fuels. However, its commercialization faces challenges due to the high costs of conventional feedstocks. This study investigated the influence of reaction parameters—catalyst concentration, reaction temperature, and reaction time—on the yield of synthesized biodiesel from waste cooking oil using snail shell and plantain peel wastes as catalysts. Snail shells were calcined at 800 °C to produce CaO and characterized by X-ray fluorescence. Organic KOH, extracted from plantain peel ash burned at 750 °C, impregnated the CaO to form a composite KOH/CaO catalyst. Using low-quality feedstock (acid value of 8.8 mg KOH/g oil), the oil underwent acid-esterification followed by transesterification under varied conditions. The optimal parameters, determined via response surface methodology (RSM), were 7% wt/wt catalyst concentration, 60.51 °C reaction temperature, and 1.93 h reaction time, achieving a maximum biodiesel yield of 92.23%. The best experimental yield, 92.10%, was obtained using a 2:1 green KOH/CaO ratio. Physicochemical properties and biodiesel composition conformed to ASTM D6751 standards. The highest fatty acid to methyl ester conversion rate, 93.86%, was achieved using the optimized snail shell catalyst. This research demonstrates that converting waste into biodiesel is not only feasible but also adds value to waste materials.

Keywords: biodiesel; heterogeneous catalysts; snail shell; plantain peel; waste cooking oil

1. Introduction

Energy is a fundamental requirement for the economic growth of every civilization. Due to its

availability and low cost, fossil-based fuels currently serve as the main source of energy, catering to the worldwide energy demand [1–3]. Recently, this demand has significantly increased due to a rapidly increasing human population and the corresponding growth of industrialization. Consequently, the currently limited reserves of fossil fuels are projected to be exhausted or depleted in the near future [4–6]. In addition to the expected price increase associated with the diminishing supply of fossil fuels, another issue of concern is the environmental impact posed by these fuels. The burning of fossil fuels accounts for more than half, or approximately 52%, of the total CO_2 emissions generated by human activities [7,8]. This greenhouse gas emission leads to ecological problems, including air pollution, ozone layer depletion, global warming as a consequence of rising global temperatures, acid precipitation, and forest destruction [9–11]. Therefore, it has become imperative to explore renewable energy sources, which are both affordable and have a lower impact on the environment [12–14].

Biodiesel, derived from organic sources or feedstocks, such as vegetable oils, waste cooking oil, or animal fats, is an environmentally friendly and sustainable replacement or alternative to fossil fuels [15–17]. Biodiesel is produced by a process known as transesterification, where the fat and vegetable or recycled oil is reacted with an alcohol, generally, ethanol or methanol, in the presence of a catalyst to yield ethyl or methyl ester biodiesel [18]. Through this process, the triglycerides in the fats or oils are converted into fatty acid ethyl or methyl ester, also known as biodiesel [19]. Compared to fossil fuels, biodiesel offers advantages as a cleaner, renewable, and sustainable alternative [15]. It is compatible with existing petrol-diesel engines with favorable lubricating properties, which can help reduce engine wear and enhance their durability [20]. Its significant growth potential makes it a desirable alternative for enhancing energy sustainability and mitigating GHG emissions [21–23]. Additionally, biodiesel emits less particulate matter and sulfur dioxide into the atmosphere, thereby enhancing air quality and lowering health hazards [24,25]. Furthermore, biodiesel offers opportunities for rural development and enhanced energy independence [26–28]. It can be generated using locally accessible feedstocks, including waste oils or agricultural products, which reduces dependency on fossil fuels and opens new business prospects to produce biofuels and farming [29,30]. One of the concerns raised by opponents of biodiesel development is the competition with food production. As such, one of the objectives of this study is the valorization of vegetable oil, plantain peel, and snail shell wastes in the production of biodiesel.

Transesterification reactions may be catalyzed using either homogeneous or heterogeneous catalysts [31]. Homogeneously catalyzed reactions often proceed at a faster rate, thereby requiring less loading when compared to heterogeneously catalyzed reactions. One of the biggest drawbacks of homogeneous catalysts is the complexity involved in the processes required for product separation and purification [32]; consequently, their reuse is often limited or even unfeasible [33]. Apart from that, it tends to create soap, which necessitates many washing processes, resulting in water consumption and the creation of emulsions in the mixture [34]. Conversely, heterogeneous catalysts exist in a phase distinct from that of the reaction mixture, allowing for simpler separation of the catalyst and eliminating the formation of soaps. This enables these catalysts to be reusable without requiring intense washing procedures, thereby minimizing process wastes and lowering overall production cost [35].

On the other hand, bio-based heterogeneous catalysts have significant benefits over conventional homogeneous catalysts in biodiesel production [36–38]. They are obtained from sustainable and renewable biomass sources, offering biodiesel producers an eco-friendly and sustainable option [39–41]. Solid-base catalysts made of organic materials, including animal bones and discarded shells of eggs, snails, and periwinkles (e.g., calcium oxide), are a typical kind of bio-based heterogeneous catalysts

used in the synthesis of biodiesel [42,43]. Obadiah et al. (2012) showed that regardless of the source of calcium oxide, the base oxide remains a suitable transesterification catalyst, being widely accessible and reasonably inexpensive [32]. Impurities in these waste-derived catalysts, however, may render them less effective than commercial CaO, and thus an alkaline support is required to increase their activity. Yang et al. (2012) [44] and other researchers explored the transesterification of vegetable oil utilizing potassium hydroxide (KOH) as a support loaded onto various oxides (MgO, CaO, Al_2O_3, kaolin, Bentonite) as heterogeneous catalysts [44–46]. It was determined that a composite catalyst of KOH/CaO produced the highest yield of biodiesel at 97.1%. Additionally, Efeovbokhan et al. (2017) documented that KOH can be extracted from plantain peel waste due to its high potassium content [47].

Therefore, this research study sets out to optimize the production of biodiesel from waste cooking oil utilizing CaO-heterogeneous catalyst synthesized from snail shells. Then, a composite catalyst of KOH/CaO derived from snail shells and plantain peel waste is employed to produce biodiesel at the obtained optimized conditions.

2. Materials and methods

2.1. Raw materials and reagents

The primary materials were sourced locally: Waste cooking oil (WCO) utilized as transesterification feedstock, plantain peel waste (PPW), and snail shell waste (SSW). The reagents used were all analaR grade: 99% purity concentrated sulfuric acid (H_2SO_4) (obtained from Sigma-Aldrich Co., UK), 99.8% purity methanol (CH_3OH) (J.T Baker Chemical Co., USA), 99.9% purity ethanol (CH_3OH) (Merck, KGaA., UK), 37% purity concentrated hydrochloric acid (Sigma-Aldrich Co., UK), potassium hydroxide pellets (KOH) (J.T Baker Co., USA), sodium hydroxide (NaOH) pellets (BDH Inc.), 99.5% purity isopropyl alcohol (Sigma-Aldrich, USA), 99% purity benzene (J.T Baker Co., USA), distilled water, phenolphthalein indicator, and methyl orange indicator.

2.2. Equipment and apparatus used

Muffle furnace, carbolite high-temperature furnace (HTF 1700) calibrated at 0–1700 °C, sample preparation sieve shaker [Biobase biodustry (Shandong) Co., Ltd], x-ray fluorescence (XRF) analyzer (Phillips PW-1800, Axios Max), air oven (Vision Scientific, Japan), gas chromatography-mass spectrometer (Varian 3800/4000, Varian Inc), hotplate magnetic stirrer (UC152, Cole-Parmer Stuart), and weighing balance (Radwag AS/310/C/2). Additionally, some of the apparatus used include 500 and 1000 mL three-neck flat bottom flasks, 250 mL conical flasks, 250 mL beakers, 500 mL measuring cylinders, 500 mL separating funnels, mercury-in-glass thermometers (0–360 and 0–110 °C), 150 mL ceramic crucibles, mortar and pestle, 50 mL burette, 25 mL pipette, glass funnel, spatula, glass stirring rods, and rubber stoppers.

2.3. Pre-treatment of WCO feedstock

WCO was filtered to eliminate solid particles such as food bits and other impurities. Afterward, the saponification value (SV), acid value (AV), and free fatty acid (FFA) content were determined

following the methods described previously [48] to ensure it was a viable feedstock for the transesterification reaction of the WCO. This is explained by the fact that a high number of FFAs (>1%) will inhibit the transesterification reaction when using an alkaline catalyst, primarily due to the formation of soap [49]. Oils with FFA content higher than 1% must undergo pretreatment by an acid esterification step to reduce the FFA content. Eqs (1–3) were used to calculate SV, AV, and FFA, respectively.

$$\text{Saponification value (SV)} = \frac{\text{Z} \times \text{M} \times 56.1}{\text{W}} \tag{1}$$

$$\text{Acid value (AV)} = \frac{\text{X} \times \text{M} \times 56.1}{\text{W}} \tag{2}$$

where Z denotes the volume of HCl used in the neutralization of excess alkali (mL), and M denotes the molarity of HCl. The average titer volume of KOH, denoted by X, is used to neutralize the solution (mL). In Eq (2), M denotes the molarity of KOH titrant, and in both Eqs (1–2), W denotes the mass (g) of WCO used, and the constant 56.10 is the molecular weight of KOH (g/mol). With the acid value known, the percentage of FFA can be determined using Eq (3):

$$\%\text{FFA} = 0.503 \times \text{AV} \tag{3}$$

With both the acid value (AV) and saponification value (SV) known, Eq (4) is applied to determine the molecular weight (M_s) of WCO [50–52]. The molecular weight is essential in establishing the masses of WCO and alcohol required to establish the alcohol-oil molar ratio desired.

$$\text{M}_\text{s} = \frac{56.1 \times 1000 \times 3}{\text{SV} - \text{AV}} \tag{4}$$

where M_s is the molecular weight of the WCO.

After the free fatty acid content was determined to be greater than 1%, an acid-esterification process was required to minimize the amount of free fatty acids within the WCO [53,54]. 300 g of WCO was weighed into a 1000 mL three-neck flat-bottom flask, and the oil was then pre-heated at a reaction temperature of 60 °C on a hotplate magnetic stirrer. In a separate 250 mL beaker, 0.6 wt/wt of methanol and 2% wt/wt of concentrated sulfuric acid (H_2SO_4) were weighed and stirred at room temperature on a separate hotplate magnetic stirrer for 5 minutes. Afterward, the methanol-acid mixture was carefully poured into the three-neck flask bearing the oil, where the mixture was allowed to react for 2 h at 65 °C and 600 rpm agitation speed. This was carried out under reflux to prevent the escape of volatile alcohol. At the end of this process, the reaction product was transferred to a separating funnel firmly secured on a retort stand. After 3 h, two distinct layers were formed. The lower layer was the esterified WCO, whereas the top layer was the acidic methanol layer, as shown in Figure 1. The esterified layer was collected in a beaker and heated to drive out water and unreacted methanol. A sample of the esterified oil was tested to ensure that the desired acid value and FFA content were achieved. Once this was confirmed, the esterified WCO was taken to the transesterification stage [55].

Figure 1. Esterified waste cooking oil.

2.4. Catalyst preparation and impregnation with organic KOH

The two catalysts prepared in this study were CaO obtained from snail shells and green KOH/CaO composite catalyst prepared from snail shells and plantain peels. The snail shells were cracked open, soaked in warm water, and washed with soap. This was repeated twice before they were then sun-dried until no moisture could be observed. The dried shells were then ground to a 75–150 μm particle size using a mechanical grinder. The ground shells were then sieved via a sieve shaker machine with a mesh size of 75 μm. After, the sieved snail shell powder was transferred into ceramic crucibles, half-full to ensure uniform heating. The crucibles were then placed in a muffle furnace and heated to 800 °C for 3 h to calcine the powder to obtain CaO, which was allowed to cool before it was placed in air-tight sample bottles and stored in a desiccator. Figure 2 shows two images of the calcination process, where (a) represents sun drying of snail shells, and (b) represents the ground calcined snail shells.

(a) (b)

Figure 2. (a) Dried snail shells and (b) calcined and ground snail shell powder.

The plantain peels were first water-washed to remove debris, food particulates, and dirt. Afterward, the peels were oven-dried in an air oven to constant weight. The now brittle plantain peels were then pounded with a mortar and pestle into a coarse powder, increasing the surface area. The plantain peel powder was then placed in 150 mL ceramic crucibles and ashed for 1 h in a muffle furnace to produce white ash. This ash was stored in a zip-lock bag and placed in a desiccator to keep it dry. The recovery of potassium hydroxide from the ash was achieved in two steps. First, 20 g of the ash was mixed with 125 mL of distilled water. The mixture was kept warm at 50 °C and stirred continuously for 1 h. The mixture was then filtered hot into a conical flask to obtain a caustic solution, confirmed by a deep blue coloration in a pH paper test. In the next step, the residue was mixed again with 50 mL of distilled water to further extract KOH. The mixture was heated to 50 °C and stirred for 1 h before it was filtered hot into a conical flask. The filtrates obtained in step 1 and step 2 were then evaporated to dryness to obtain solid KOH, which was then weighed and kept in plastic containers stored in a desiccator to keep dry [47].

The alkalinity of organic KOH in terms of hydroxide and carbonates present was determined by the double-indicator titration method [56,57]. 1 g of organic KOH was dissolved in 25 mL of distilled water in a 250 mL conical flask. The solution was then titrated with 0.5 N H_2SO_4 using three drops of phenolphthalein indicator (endpoint indicated when the pale pink coloration turned colorless). Following this, three drops of methyl orange indicator were added to the solution, which was then further titrated with 0.5 N H_2SO_4 (endpoint indicated when the yellow coloration turned reddish pink). The volumes of titrant (0.5 N H_2SO_4) used in the sequential titrations were recorded and used in Eqs (5–6) to calculate the hydroxide alkalinity and carbonate alkalinity of the synthesized organic KOH.

Equation 5 was used to determine the percentage purity of alkali constituents (hydroxides and carbonates) and non-alkali components present in the given sample.

$$\%purity\ of\ constituent = \frac{mass\ of\ constituent}{total\ sample\ mass} \times 100 \tag{5}$$

where the mass of the constituent is determined using a combination of Eqs (6–9) as well as stoichiometric analysis.

$$\text{Number of moles of acid used to neutralize hydroxide } = n_1 = cv_1 \tag{6}$$

$$\text{Number of moles of acid used to neutralize carbonate } = n_2 = cv_2 \tag{7}$$

$$v_1 = 2P - M \tag{8}$$

$$v_2 = 2(M - P) \tag{9}$$

where c denotes the concentration of acid (mole/L), v_1 denotes the volume of titrant used to neutralize hydroxide (mL), v_2 denotes the volume of titrant used to neutralize carbonate (mL), P denotes the burette reading at phenolphthalein end point (mL), and M denotes the burette reading at methyl orange end point (mL).

The KOH/CaO composite catalyst was prepared in three molar ratios of 1:2, 1:1, and 2:1 by incipient wetness impregnation. 5.00, 10.01, and 20.01 g of organic KOH were weighed, and each was separately dissolved in 70 mL of distilled water to form three solutions. Afterward, 10 g of snail shell-derived CaO was suspended in each aqueous solution of organic KOH and stirred continuously for 1 h. The mixtures were each heated at 150 °C for 4 h to drive off moisture before being calcined

at 500 °C for 1 h in a muffle furnace. The synthesized catalysts were labeled as CCB for a molar ratio of 1:2 (KOH:CaO), CCA for a molar ratio of 1:1 (KOH:CaO), and CCC for a molar ratio of 2:1 (KOH:CaO), before they were kept in airtight plastic containers and stored in desiccators to keep conditions dry.

2.5. Experimental design

Experimental data collected were statistically analyzed utilizing response surface methodology (RSM) using MINITAB 20 software. Of the available response surface methodologies, the Box-Behnken design was selected and used in ascertaining the number of experimental runs necessary to study the influence of varied operating parameters on biodiesel yield [58]. Tables 1 and 2 show the coded and varied parameters, respectively, which include catalyst concentration (%wt/wt), coded A, reaction temperature (°C), coded B, and reaction time (h), coded C.

Table 1. Box-Behnken design displaying coded factors and their respective levels.

Factor	Unit	Symbol	Level		
			Low (−1)	Middle (0)	High (1)
Catalyst concentration	% wt/wt	A	2	4.5	7
Reaction temperature	°C	B	50	60	70
Reaction time	h	C	1	1.5	2

Table 2. Box-Behnken design of varied reaction parameters in WCO transesterification.

Run	Catalyst concentration (% wt/wt)	Reaction temperature (°C)	Reaction time (h)
1	2	50	1.5
2	7	70	1.5
3	4.5	70	2
4	2	70	1.5
5	7	60	1
6	4.5	60	1.5
7	7	50	1.5
8	4.5	70	1
9	4.5	60	1.5
10	4.5	50	1
11	2	60	1
12	4.5	60	1.5
13	2	60	2
14	7	60	2
15	4.5	50	2

The response surface generated was analyzed and subsequently optimized using the design of experiment (DOE) response optimizer in MINITAB 20. Using a full quadratic model, the mathematical interrelation between biodiesel yield (as a dependent variable) and the three varied factors (independent variables) was established.

Yield as a function of the parameters is expressed by the general formula of a second-order response surface model, as expressed in Eq (10).

$$Y = \alpha_o + \alpha_1 A + \alpha_2 B - \alpha_3 C - \alpha_{11} A \times A + \alpha_{22} B \times B - \alpha_{33} C \times C + \alpha_{12} A \times B + \alpha_{13} A \times C - \alpha_{23} B \times C \quad (10)$$

Y denotes the predicted biodiesel yield (%), α_o denotes the intercept, α_1, α_2, and α_3 denote linear coefficients, α_{12}, α_{13}, and α_{23} depict the interactive regression coefficients, α_{11}, α_{22}, and α_{33} are the quadratic coefficients, and A, B, and C denote coded factors of the model.

For all runs, stirring speed was held constant at 600 rpm, and the methanol to oil molar ratio was held constant at 9:1.

MINITAB 20 (LEAD Technologies, Inc., Minneapolis, MN, USA) was utilized to create a regression model and interaction surface plots for the experimental data recorded. The optimum conditions required to maximize the biodiesel yield from calcined snail shell catalyzed transesterification of WCO were determined using MINITAB 20 software.

2.6. Transesterification of waste cooking oil

100 g of acid esterified WCO was heated to 110 °C until no visible signs of water could be observed. This was then confirmed by conducting a splatter test. 75 g of the dried esterified WCO was then poured into a 500 mL three-neck flat-bottom flask and maintained at the preselected reaction temperature. In a 250 mL beaker, the appropriate mass of methanol (methanol:oil molar ratio of 9:1) was mixed with the appropriate mass concentration of catalyst for 15 minutes. The methanol-catalyst mixture was then carefully transferred into the three-neck flat-bottom flask containing the esterified WCO and allowed to react for the appropriate reaction time under reflux. A thermometer was inserted into one neck to keep track of the temperature, while the other neck was corked to prevent the escape of methanol. The reaction time, reaction temperature, and catalyst concentrations were determined by the design of experiment.

After the required amount of reaction time had elapsed, the reaction was stopped, and the flask was removed from the hotplate stirrer and left to stand for 1 h. This allowed the catalyst to settle at the base of the flask to prevent clogging of the separating funnel. After, the product mixture was decanted into a separating funnel and left for 24 h to allow for adequate separation. Three layers were observed: a top layer of unreacted methanol, a middle layer composed of biodiesel, and a bottom glycerol layer containing residual catalyst. The biodiesel layer was then collected in a beaker and heated at 65 °C until no methanol could be observed. The biodiesel yield, based on mass, was calculated with Eq (11).

$$\%\text{Biodiesel yield} = \frac{\text{weight of biodiesel}}{\text{weight of WCO fed}} \quad (11)$$

The same procedure was followed in producing biodiesel using both the heterogeneous CaO catalyst and the heterogeneous composite KOH/CaO catalysts.

2.7. Biodiesel and catalyst characterization

The physicochemical properties of WCO and WCO biodiesel produced using both CaO from calcined snail shell (CSS) and the various composite catalysts (CCA, CCB, and CCC) derived from

differing molar ratios of green KOH/CaO blends were conducted. The biodiesel properties including density, kinematic viscosity, specific gravity, acid value, cloud point, pour point, and flash point were obtained following established test procedures of the American Society for Testing and Materials (ASTM) standard for biodiesel qualities (ASTM D6751). The specific fatty acids contained in the WCO, as well as the resulting fatty acid methyl esters in the WCO biodiesel, were analyzed via gas chromatography-mass spectrometry.

X-ray fluorescence (XRF) analysis of the calcined snail shell catalyst was conducted to ascertain the chemical composition of major oxides present in the catalyst. This was to ensure that enough calcium oxide was obtained by the calcination of snail shells at a temperature of 800 °C for a holding time of 3 h in a muffle furnace

3. Results and discussion

3.1. Catalyst characterization

Table 3 shows the X-ray fluorescence analysis of calcined snail shell catalyst derived by calcination of snail shells (CSS) at 800 °C for 3 h. The analysis of the CSS confirms the presence of 84.02% CaO as well as other metallic oxides in smaller compositions. The catalyst also contains a significant amount of MgO at 3.05%. Some researchers have observed that the combination of oxides of alkali earth metals, such as CaO and MgO, synergistically modifies the electronic properties of catalyst surfaces [59–61], leading to a larger number of basic sites in contrast to the number observed in single metal oxide catalysts. Hence, MgO may improve the performance of the catalyst, rather than hinder it as an impurity.

Table 3. X-ray fluorescence spectrometry of calcined snail shell catalyst.

Compound	Composition (%)
SiO_2	4.2
AI_2O_3	2.5
Fe_2O_3	2.25
MnO	0.4
CaO	84.02
P_2O_5	0.75
K_2O	0.53
TiO_2	0.35
SO_3	1.02
Na_2O	0.002
MgO	3.05
Cl	0.26
LOI	0.8
RbO	0.03
ZnO	0.1
Cr_2O_3	0.01
SrO	0.02

3.2. Analysis of alkalinity and percentage purity of organic KOH constituents

Table 4 lists the alkalinity and contribution to total alkalinity of the hydroxide and carbonate constituents found in synthesized organic KOH. The result shows that the carbonate and hydroxide constituents of the sample have a contribution of 95.66% and 4.34%, respectively, to total alkalinity. As carbonates are known to be weaker bases than hydroxides, a larger contribution of carbonates to total alkalinity indicates that a significantly larger amount of carbonate exists in the sample. This is confirmed in Table 5, which lists the percentage purity of suspected constituents of the synthesized sample. Hydroxide, carbonate, and non-alkali constituents were found to have a purity of 3.31%, 72.9%, and 23.79%, respectively, indicating that most of the sample mass is made of potassium carbonate. This indicates that a calcination temperature of 750 °C combined with a holding time of 1 h is insufficient for complete degradation of plantain peel carbonates to their oxides. Also, a significant purity of non-alkali indicates the existence of non-alkali soluble salts within the sample.

Table 4. Hydroxide and carbonate alkalinity and contribution to total alkalinity.

Alkali constituent	Alkalinity (mg/L)	Contribution to total alkalinity (%)
KOH	1324.09	4.34
K_2CO_3	29161.26	95.66

Table 5. Percentage purity of organic KOH constituents.

Constituent	Percentage purity (%)
KOH	3.31
K_2CO_3	72.9
Non-alkali	23.79

According to Ofori and Awudza (2017), of the soluble carbonates found in plantain peel ash, potassium carbonate occurs in a significantly large amount compared to sodium carbonate. Hence, the sample is most likely primarily potassium carbonate, with negligible amounts of sodium carbonate [62].

3.3. Comparability of experimental yield and calculated yield

Table 6 shows the experimental design results obtained using the Box-Behnken design of Minitab 20 software. This design determined the required number of experimental runs to explore the effects of varied reaction parameters (catalyst concentration, reaction temperature, and reaction time) on biodiesel yield (response). From the table, the experimental and calculated yields of biodiesel produced from CSS can be compared. The comparison shows minimal deviations, indicating that the regression equation generated was influential in determining the expected yield of biodiesel. Deviations between the experimental yield and calculated yield are mostly observed in experimental runs having a larger amount of catalyst concentration (7%). A likely cause of this is the difficulty in product separation resulting from the high amount of catalyst present in the reaction mixture, which may clog the separating funnel. As noted by other researchers, product separation is also made difficult by high-viscosity reaction mixtures [17,63]. A high concentration of the solid catalyst results in a

denser consistency and increases its adherence to the walls of the flasks or separating funnels. This results in product loss, contributing to higher deviations (lower experimental yields) seen between experimental and calculated results for runs using a 7% wt/wt catalyst concentration.

Table 6. Results of Box-Behnken experimental design.

Run order	Catalyst concentration (% wt/wt)	Reaction temperature (°C)	Reaction time (h)	Experimental yield using CSS (%)	Calculated yield using CSS (%)
1	2	50	1.5	66.53	69.52
2	7	70	1.5	82.75	79.77
3	4.5	70	2	79.31	77.96
4	2	70	1.5	65.20	67.14
5	7	60	1	82.01	82.61
6	4.5	60	1.5	85.49	86.15
7	7	50	1.5	85.73	83.79
8	4.5	70	1	63.82	66.20
9	4.5	60	1.5	86.27	86.15
10	4.5	50	1	75.06	76.41
11	2	60	1	79.23	74.90
12	4.5	60	1.5	86.70	86.15
13	2	60	2	74.53	73.92
14	7	60	2	88.77	93.11
15	4.5	50	2	76.55	74.16

3.4. Statistical analysis of variance for CSS-catalyzed transesterification

The regression in Eq 12, generated by Minitab 20 at a 95% confidence level, was determined to have an R-square value of 0.9149. The R-squared value is a statistical measure that explains the extent to which the variation of an independent variable(s) accounts for the variations in a dependent variable within a regression model. The R-sq value obtained indicates that 91.49% of the combined influences of reaction parameters (catalyst concentration, reaction temperature, and reaction time) on the yield of biodiesel obtained in the CSS catalyzed process can be explained by the variations in parameters used.

The p-value and F-value of the CSS catalyzed process model were 0.032 and 5.97, respectively, as observed in Table 7. Based on the p-value obtained, the model is significant for a confidence level of 95% (p-value lower than 0.05). This implies that the developed model is statistically significant and adequately depicts the relationship between reaction parameters and product yield.

Table 7. Statistical analysis of results obtained from the Box-Behnken design.

Source	Df	Adj SS	Adj MS	F-value	p-value	Remarks
Model	9	853.728	94.859	5.97	0.032	Significant
Linear	3	427.297	142.432	8.97	0.019	Significant
A: Catalyst conc.	1	361.555	361.555	22.77	0.005	Highly significant
B: Reaction temp	1	20.466	20.466	1.29	0.308	Insignificant

Continued on next page

Source	Df	Adj SS	Adj MS	F-value	p-value	Remarks
C: Reaction time	1	45.277	45.277	2.85	0.152	Insignificant
Square	3	343.809	114.602	7.22	0.029	Significant
AA	1	12.277	12.277	0.77	0.420	Insignificant
BB	1	317.700	317.700	20.00	0.007	Highly significant
CC	1	37.675	37.675	2.37	0.184	Insignificant
2-way interaction	3	82.624	27.541	1.73	0.275	Insignificant
AB	1	0.673	0.673	0.04	0.845	Insignificant
AC	1	32.907	32.907	2.07	0.210	Insignificant
BC	1	49.043	49.043	3.09	0.139	Insignificant
Lack-of-fit	3	78.653	26.218	69.52	0.014	Significant
Pure error	2	0.754	0.377	-	-	

- R-sq = 0.9149
- R-sq(adj) = 0.7617

3.5. Effects of interacting reaction parameters on biodiesel yield

Utilizing the response surface methodology on Minitab 20, 2D surface plots were generated to study the effects of selected pairs of parameters (while holding a third parameter constant) on the WCO biodiesel yield obtained using a CSS catalyst.

Figure 3 illustrates the relationship between reaction temperature and catalyst concentration while the reaction time is held constant at a middle value (1.5 h). The yield plot illustrates that the yield of biodiesel increases as both the reacting temperature and catalyst concentration increase. As the quantity of catalyst increases, the consistency of the reacting mixture increases, reducing the yield of the reaction [64]. However, the yield plot shows that as temperature and catalyst concentration increase, the subsequent biodiesel yield increases as well. This is because of two reasons: first, as the temperature of the reacting oil increases, its viscosity is reduced [65]. This means that the reduction in viscosity brought about by the increase in temperature is enough to compensate for the increase in viscosity arising from high catalyst loading. Second, as more heat is applied, reactants gain more kinetic energy and subsequently increase the frequency of collisions with the catalytically active sites [66,67].

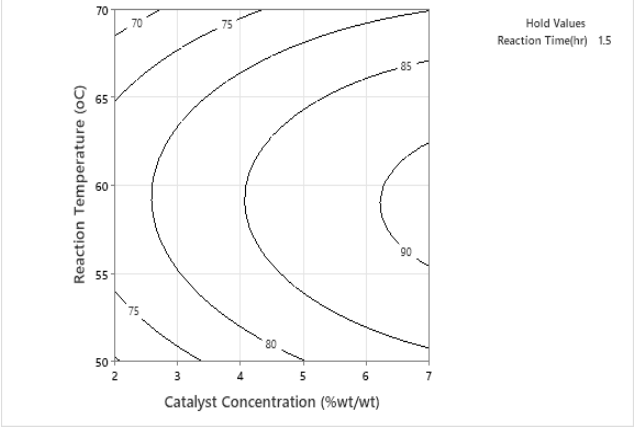

Figure 3. Effect of reaction temperature and catalyst concentration on biodiesel yield.

Figure 4 depicts the interrelation between reaction time and catalyst concentration and yield of biodiesel, while the reaction temperature is maintained evenly between the high and low levels (a middle level of 60 °C). From the plot, it can be observed that at low reaction times of about 1–1.1 h, an increment in catalyst concentration from 2% to 7% wt/wt increases biodiesel yield at a minimal rate. This is because a higher catalyst loading increases the viscosity or consistency of the reaction mixture, which, in turn, causes ineffective mass transfer and restricts reactants' access to the catalyst's active sites [68]. This process is then improved by the increase in reaction time, which then provides more time for the reactants to interact on the catalyst before the reaction is stopped, hence increasing the yield. This is consistent with the findings of Faruque et al. (2020) [69], which postulated that heterogeneous catalysts require more time to reach optimum biodiesel yield. Hence, at higher reaction times of 1.5–2 h and high catalyst concentrations of 6%–7% wt/wt, the highest yields of biodiesel can be achieved (>90%).

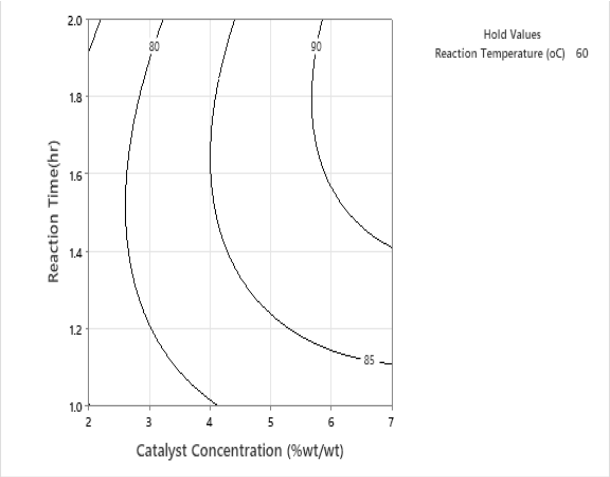

Figure 4. Effect of reaction time and catalyst concentration on biodiesel yield.

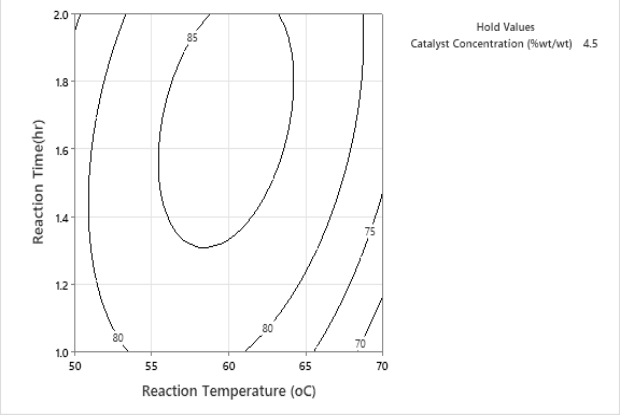

Figure 5. Effect of reaction temperature and reaction time on biodiesel yield.

Figure 5 illustrates the relationship between reaction time and reaction temperature while holding catalyst concentration at its middle level (4.5%) using the Box-Behnken design of Minitab 20. The

yield plot shows that as time increases, a higher reaction temperature is required to achieve yields of above 85%. This is likely due to the reversibility of the reaction. According to Ismail et al. (2016) [70], at lower reaction times, the production of biodiesel is rapid until an equilibrium point is reached, wherein the reverse reaction begins to occur. At this point, higher reaction temperatures are required to drive the forward reaction to increase biodiesel yield. Further inspection of the plot indicates that at high reaction temperatures and low reaction times, the yield reduces drastically to below 70%. This can be attributed to a combination of two reasons. First, at temperatures beyond 65 °C (the temperature at which methanol boils at atmospheric conditions), methanol begins to bubble, reducing the number of interactions between reactants and the catalyst, thus reducing biodiesel yield [70]. Also, reaction times of 1 h are insufficient for the effective transesterification using heterogeneous catalysts [71].

3.6. Optimization of the transesterification of WCO using CSS catalyst

The design of experiment (DOE) response optimizer on Minitab 20 software was utilized to identify the optimal conditions required to achieve the maximum biodiesel yield obtained from the transesterification of WCO. The optimal point was obtained at 7% wt/wt catalyst concentration, 60.5051 °C, and a 1.9293 h reaction time to obtain a theoretical WCO biodiesel yield of 93.23%. The experimental yield at these conditions was 88.77%, as shown in Table 8.

Table 8. Yield of biodiesel produced using catalysts at optimum conditions.

S/N	Catalyst used	Designation	KOH:CaO molar ratio	Biodiesel yield (%)
1	Calcined snail shells	BCSS		88.77
2	Composite catalyst B	BCCB	1:2	91.55
3	Composite catalyst A	BCCA	1:1	90.58
4	Composite catalyst C	BCCC	2:1	92.10

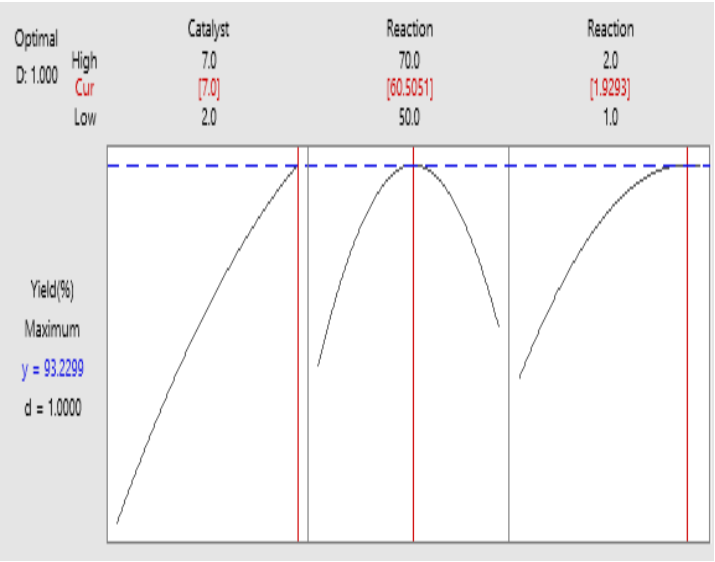

Figure 6. Optimization of WCO biodiesel yield using CSS catalyst.

Figure 6 depicts optimum conditions obtained from the response optimizer in Minitab 20 to

maximize the yield of biodiesel. An optimal catalyst concentration of 7% wt/wt indicates that the increase in catalyst concentration from 2% to 7% favors the yield of biodiesel. This occurs without reaching a plateau, indicating that this amount of catalyst does not significantly increase the viscosity of the reaction mixture to a detrimental level.

An optimal reaction temperature of 60.5051 °C indicates that as the temperature increases to 70 °C, the methanol bubbles rapidly, which prevents proper mixing of the reactants. This aligns with the findings from other researchers [72], who observed that at a temperature exceeding the saturation temperature of methanol (64.7 °C), product yield is negatively affected as a result of alcohol loss through vaporization.

An optimal reaction time of 1.9293 h implies that an increase in reaction time favors the forward reaction until a point is reached where the plot begins to plateau. At this point, it is likely that the reverse of the transesterification reaction begins to occur. This finding is consistent with the results reported by Animasaun et al. (2021) [73], who stated that biodiesel yield achieved via base-catalyzed transesterification is highest when the reaction duration is kept below 120 minutes (2 h). The combination of these optimum conditions produces a WCO biodiesel yield of 93.23%.

3.7. Comparison of biodiesel yield using synthesized catalysts at optimum conditions

The optimum conditions determined from the Box-Behnken DOE were used to produce biodiesel using composite catalysts B, A, and C, which were prepared from the wet impregnation of organic KOH on calcined snail shell catalyst (CSS) at molar ratios of 1:2, 1:1, and 2:1. The yields of biodiesel produced are compared in Table 8.

Figure 6 indicates that as the amount of organic KOH (Or.KOH) doped onto the CSS increases to a molar ratio of 1:2, the biodiesel yield increases, most likely as a result of an increase in alkalinity. As the amount of Or.KOH increases to a molar ratio of 1:1, the yield reduces, most likely due to the excess KOH loading, which blocks the active sites of the CSS component. This complies with findings of Yang et al. (2012) [44]: as KOH loading on the CaO catalyst increases beyond 15%, product yield begins to decrease. As the amount increases further to a molar ratio of 2:1, the yield of biodiesel begins to increase again. When a large amount of KOH is doped onto the catalyst, a large amount of soap is subsequently formed along with moisture. The mass of this moisture may significantly contribute to the weight of biodiesel and hence the perceived yield achieved.

3.8. Variations in physicochemical properties of WCO and biodiesel produced

The density of fuel influences the quality of combustion in an engine because many diesel fuel engine systems are designed and metered based on a predetermined volume. The density of fuel alters the weight of fuel that reaches the combustion chamber and, therefore, the performance of the engine. It is, therefore, necessary that a fuel has a density within a specified standard range. Table 9 shows that the feedstock (WCO) has a density of 0.907 g/cm^3 at 30 °C, exceeding the ASTM standard, whereas all produced biodiesel samples fall within the standard density range 0.86–0.89 g/cm^3. The biodiesel produced using the CCA catalyst had the lowest density at 0.86 g/cm^3, whereas the biodiesel produced using the CSS catalyst had the highest density at 0.87 g/cm^3. The specific gravity of each biodiesel sample is directly proportional to its density; hence, the same trend is observed.

Table 9. Physicochemical properties of biodiesel produced compared with ASTM standards.

S/N	Properties	WCO	BCSS	BCCB	BCCA	BCCC	ASTM standard	
1	Density (g/cm^3) (30 °C)	0.907	0.879	0.869	0.859	0.868	0.86–0.89	ASTMD6751
2	Specific gravity (30 °C)	0.911	0.883	0.873	0.867	0.872	0.86–0.9	ASTMD6751
3	Kinematic viscosity (mm^2/s) (40 °C)	21.206	3.349	2.142	1.981	2.306	1.9–6.0	ASTMD6751
4	FFA content (mg/g)	4.430	0. 240	0.074	0.064	0.092	1.0 max	ASTMD6751
5	Acid value (mg KOH/g)	8.808	0.478	0.147	0.126	0.182	0.8 max	ASTMD6751
6	Cloud point (°C)	7	10	11	12	12	−15 to −5	ASTMD975
7	Pour point (°C)	0	5	4	5	5	−35 to −15	ASTMD975
8	Flash point (°C)	260	160	154	138	118	60 min	ASTMD975

where
Min: minimum;
Max: maximum;
BCSS: optimum biodiesel using calcined snail shell catalyst;
BCCA: optimum biodiesel using composite catalyst A;
BCCB: optimum biodiesel using composite catalyst B;
BCCC: optimum biodiesel using composite catalyst.

The acid value is a number that quantifies the rancidity of biodiesel, as the free fatty acids that constitute this value are typically formed as a result of the decomposition of triglycerides. Hence, it is a noteworthy property of any biodiesel sample. The acid value of WCO decreased significantly from 8.808 to 0.478, 0.126, 0.147, and 0.182 mg KOH/g when using the CSS, CCA, CCB, and CCC catalysts, respectively. From this, it can be seen that the composite catalysts, most likely due to their high alkalinity, have the capacity to significantly lower the acid value of WCO to values lower than those achieved using the calcined snail shell catalyst. It can be noted that the increment in the amount of KOH loading reduces the acid value to a minimum point (molar ratio of 1:1 of KOH:CaO). Beyond this point (2:1 molar ratio KOH:CaO), the acid value increases, most likely as a result of excess KOH lowering the number of active sites available in the CaO component. Thus, the catalytic ability to lower the acid value of the biodiesel is hindered. A matching trend is observed when comparing the amount of FFA present in the biodiesel samples prepared, as FFA content is directly proportional to acid value.

The kinematic viscosity of a liquid measures its resistance to flow, brought on by internal friction as portions of liquid move over one another. Highly viscous fuels tend to stick to walls, grooves, and internal parts of the engine, leaving unburned oxidized fuel to build up and cause further damage within the engine. The viscosity of WCO was found to be 21.206 mm^2/s, whereas the viscosities of the biodiesel produced were 3.349, 1.981, 2.141, and 2.306 mm^2/s when using the CSS, CCA, CCB, and CCC catalysts, respectively. This shows a dramatic reduction in kinematic viscosity, indicating a high conversion of free-fatty acids to FAMEs. The viscosities obtained from the catalyzed transesterification reaction all lay within the ASTM standard specifications. As with the density and acid value, the lowest kinematic viscosity (1.981 mm^2/s) was observed with the CCA catalyst, which indicates that the increase in KOH loading during impregnation of the CSS results in an increase in reduction of oil viscosity. When the amount of KOH loaded is increased beyond this point (1:1 molar ratio), the viscosity begins to increase. This may be as a result of the excess KOH obscuring the active sites of the CaO component, reducing the catalytic activity. Also, the excess amount of KOH contributes to more soap formation, hindering the transesterification process.

According to some researchers [74,75], the cloud point is the temperature below which crystals of bio-wax begin to form in biodiesel, forming a cloudy appearance. This solidified wax can thicken the biodiesel and clog injectors in engines. Therefore, the cloud point depicts the propensity of the biodiesel to clog small apertures when used in cold climates. The cloud point of WCO and the biodiesel produced using CSS, CCA, CCB, and CCC catalysts was 7, 10, 12, 11, and 12 °C. This indicates that the amount of KOH loading during the impregnation of CSS has little to no effect on the cloud point.

Furthermore, it can be observed that the cloud point is inversely proportional to density, with the WCO having the highest density but the lowest cloud point. This is in compliance with findings from Maheshwari et al. (2012) [76], who postulated that density reduction implies an increase in the presence of paraffins. Fuels rich in n-paraffinic components, such as dodecane (present in the biodiesel samples produced as seen in Table 11), crystallize more rapidly, resulting in higher pour and cloud points.

After the cloud point is reached, further cooling results in the formation of a crystal network of paraffins in the fuel, which renders it incapable of flowing; this is known as the pour point. The pour point is directly proportional to the cloud point; hence, a similar trend is observed with the WCO and the biodiesels produced using CSS, CCA, CCB, and CCC catalysts having pour points of 0, 5, 5, 4, and 5 °C.

These two qualities measure the biodiesel's cold flow properties and indicate the fuel's ability to operate in cold climates. In tropical regions such as Nigeria, the high values obtained may not reduce the performance of these fuels in regular conditions.

The flash point temperature represents the minimum temperature at which a fuel releases ignitable vapors, which briefly ignite in the presence of a fire source. The WCO feedstock has a flash point of 260 °C, which, although safe, requires much more thermal energy to produce ignitable vapors as compared to regular diesel (50 °C flash point). The transesterification of WCO at optimum conditions using CSS resulted in reducing the flash point from 260 to 160 °C, which is between the acceptable temperatures specified by the ASTM. A high flash point of 160 °C indicates that the generated biodiesel is suitable for storage and use as the fuel is not able to ignite at relatively low temperatures. Also, the flash point of biodiesel produced lowers (154, 138, and 118 °C) as the amount of KOH doping increases. Although this means that less thermal energy will be required to use biodiesel as a fuel, it also means that additional precautions must be taken for safe storage.

3.9. Comparison of gas chromatography-mass spectrometry results

Tables 10 and 11 show the results obtained by gas chromatography-mass spectrometry analysis of WCO and its biodiesel samples, respectively. Observing Table 10, it can be noted that WCO primarily contains free fatty acids, having a 90.16% wt acid content. Table 11 shows that the biodiesel produced is made primarily of fatty acid methyl esters. Our results are consistent with the findings of several other researchers who have shown that the acids found in waste cooking oil can be converted into fatty acid methyl esters using heterogeneous base catalysts [77–80].

Table 11 shows that the different total ester contents of biodiesel produced using CSS, CCB, CCA, and CCC catalysts were 84.62%, 84.18%, 83.42%, and 81.29%. From these values, the conversion of fatty acids to FAMEs achieved by each catalyst was obtained. The results indicate that the conversion achieved for the CSS, CCB, CCA, and CCC catalysts was 93.86%, 91.15%, 92.52%, and 90.16% respectively. By comparing the achieved conversions, it can be observed that the CSS catalyst bearing

no organic KOH converts the largest amount of acid to FAMEs (93.86% conversion), whereas the CCC catalyst converts the least amount of acid to FAMEs (90.16% conversion). Hence, an increase in the amount of KOH doped onto the CSS catalyst results in a decrease in ester formation. From Table 8, the catalysts developed in this study—calcined snail shell (CSS) and CSS doped with varying molar concentrations of KOH (CCB, CCA, CCC)—achieved biodiesel yields of 88.77%, 91.55%, 90.58%, and 92.10%, respectively. These results match those of Kedir et al. (2023) [81], who reported 80% biodiesel yield using snail shell-derived CaO, which increased to 90% and 95% upon modification with ZnO and TiO_2, respectively. The high biodiesel yields obtained in this study highlight the efficacy of the developed green catalysts and their prospective potential for sustainable production of biodiesel.

Table 10. Results of gas chromatography-mass spectrometry analysis of WCO.

S/N	Compound name	Molecular formula	Compound weight
1	3-Hexen-1-ol	$C_6H_{12}O$	2.85
2	Cyclohexaneethanol	$C_8H_{16}O$	2.93
3	9,12,15-Octadecatrienoic acid, (Z,Z,Z)-	$C_{12}H_{24}O_2$	1.38
4	Methyl tetradecanoate	$C_{15}H_{30}O_2$	1.46
5	Oleic acid	$C_{18}H_{34}O_2$	1.53
6	trans-13-Octadecenoic acid	$C_{18}H_{34}O_2$	0.47
7	cis-10-Heptadecenoic acid	$C_{17}H_{32}O_2$	1.08
8	Heptadecanoic acid	$C_{17}H_{34}O_2$	1.29
9	9-Hexadecenoic acid	$C_{16}H_{30}O_2$	0.86
10	9,12-Octadecadienoic acid (Z,Z)-	$C_{18}H_{32}O_2$	19.26
11	n-Hexadecanoic acid	$C_{14}H_{28}O_2$	10.15
12	Octadecanoic acid	$C_{18}H_{36}O_2$	15.99
13	14-methylpentadecanoic acid	$C_{16}H_{32}O_2$	30.21
14	11-Octadecenoic acid, (Z)-	$C_{18}H_{34}O_2$	5.32
15	Methyl stearate	$C_{19}H_{38}O_2$	2.51
16	cis-11-Eicosenoic acid	$C_{20}H_{38}O_2$	1.80
Total unresolved compound weight (% wt)			0.91
Total known compound weight (% wt)			99.09
Total acid content (% wt)			90.16

Deeper inspection of Table 11 shows that the reduction in conversion to FAMEs occurs with an increase in conversion of WCO to the hydrocarbons exo-tricyclo ($5.2.1.0^{2.6}$) decane and dodecane. This phenomenon can be explained by the increase in the amount of KOH doped onto the catalyst, which may serve as a catalyst or reactant in the complex hydrocarbon-producing side reactions that occurred. The other reactants involved in this complex side reaction may include the 3-hexen-1-ol impurity present in the WCO, amorphous impurities existing in the organically derived KOH, and the unresolved compounds present in the biodiesel. Although these hydrocarbons can be viewed as impurities in the biodiesel, the two compounds are currently used in the production of jet fuels [81].

According to Li et al. (2019) [81], exo-tricyclo($5.2.1.0^{2.6}$)decane is currently used in missiles and supersonic military jets as a super fuel (JP-10 fuel) because of its high-energy density and good thermal stability. Additionally, Kim et al. (2017) [82] posited that dodecane can serve as a surrogate for kerosene-based jet fuels. Hence, the hydrocarbon by-products may serve to improve the fuel

characteristics and engine performance of the biodiesel rather than hinder them.

Table 11. Gas chromatography-mass spectrometry analysis of optimum biodiesel produced.

S/N	Compound name	Molecular formula	Compound weight (%)			
			BCSS	BCCB	BCCA	BCCC
1	Exo-tricyclo(5.2.1.$0^{2.6}$)decane	$C_{10}H_{16}$	10.91	10.21	10.51	6.32
2	Dodecane	$C_{12}H_{26}$	2.95	3.53	3.80	9.53
3	Cyclohexaneethanol	$C_8H_{16}O$	1.48	2.70	2.24	1.89
4	8,11-Octadecadienoic acid, methyl ester	$C_{19}H_{34}O_2$	17.00	17.33	17.66	16.25
5	9-Hexadecenoic acid, methyl ester, (Z)-	$C_{17}H_{32}O_2$	1.85	2.60	1.58	2.32
6	Dodecanoic acid, methyl ester	$C_{13}H_{26}O_2$	2.63	2.46	2.13	2.41
7	Pentadecanoic acid,13-methyl ester	$C_{16}H_{32}O_2$	4.99	4.76	2.95	3.21
8	Methyl tetradecanoate	$C_{15}H_{30}O_2$	1.50	1.21	1.17	2.04
9	9,12,15-Octadecatrienoic acid, methyl ester	$C_{19}H_{32}O_2$	2.11	1.35	1.81	0.94
10	9-Octadecenoic acid, methyl ester	$C_{19}H_{36}O_2$	13.09	14.21	14.57	13.17
11	Hexadecanoic acid, methyl ester	$C_{17}H_{34}O_2$	5.94	5.32	5.63	5.21
12	Tridecanoic acid, methyl ester	$C_{14}H_{28}O_2$	6.73	6.01	6.00	5.83
13	Docosanoic acid, methyl ester	$C_{23}H_{46}O_2$	20.72	20.18	22.08	22.15
14	Eicosanoic acid, methyl ester	$C_{21}H_{42}O_2$	3.98	3.51	3.61	3.62
15	Methyl stearate	$C_{19}H_{38}O_2$	2.03	2.00	2.31	2.21
16	Tetracosanoic acid, methyl ester	$C_{25}H_{50}O_2$	1.83	1.24	1.92	1.93
Unresolved compound weight (% wt)			0.26	1.38	0.03	0.97
Total known compound weight (% wt)			99.74	98.62	99.97	99.03
Total ester content (% wt)			84.62	82.18	83.42	81.29
Total conversion of fatty acid to FAME (%)			93.86	91.15	92.52	90.16

4. Conclusions

This study successfully demonstrates that waste materials such as snail shells and plantain peels can be effectively used as catalysts in the production of biodiesel from waste cooking oil. The study presents a viable method for producing biodiesel, helping to reduce greenhouse gas emissions and dependence on fossil fuels.

The key findings in this study and their implications are summarized below:

- Snail shells and plantain peels were successfully utilized as catalysts in the production of biodiesel from waste cooking oil.
- This approach offers a greener and more affordable alternative to conventional catalysts, which are often costly, environmentally harmful, and unsustainable.
- Using response surface methodology (RSM) and Box-Behnken design, optimal conditions were determined as follows: 7% wt/wt catalyst concentration, 60.51 °C reaction temperature, and 1.93 h reaction time, resulting in 92.23% maximum biodiesel yield.
- The biodiesel produced met ASTM D6751 standards, confirming its suitability for diesel engines without modification.
- Repurposing waste materials helps reduce environmental impact and supports sustainable energy practices.

Limitations and future work

While the success achieved in the laboratory indicates potential for large-scale production of biodiesel using CaO/KOH biocomposites derived from biomass materials, there are still several limitations to contend with, highlighting the need for further studies to address some of the practical challenges encountered. These include:

- Optimization of KOH content in the plantain peel extract to minimize the presence of sodium carbonate, which may affect catalyst purity and performance.
- Enhancement of catalyst potency, particularly the activity and stability of the CaO/KOH biocomposite, to improve reaction efficiency.
- Development of effective separation and recovery techniques to enable catalyst reuse without significant loss of activity.
- Assessment of catalyst life cycles, including performance across multiple reaction cycles and long-term durability under operational conditions.

Use of AI tools declaration

The authors declare they have not used Artificial Intelligence (AI) tools in the creation of this article.

Acknowledgments

This work was supported by [Covenant University, Ota]. They provided the enabling environment and paid the article processing charges.

Conflict of interest

The authors declare no conflict of interest.

Author contributions

All authors contributed to the study conception and design. Material preparation, data collection and analysis were performed by Vincent E Efeovbokhan, Ubong E. Usoro, Omololu Fagbiele and Olubunmi G. Abatan. The first draft of the manuscript was written by Vincent E Efeovbokhan and Ubong E. Usoro and all authors commented on previous versions of the manuscript. All authors read and approved the final manuscript.

References

1. Ebhota WS, Jen TC (2020) Fossil fuels environmental challenges and the role of solar photovoltaic technology advances in fast tracking hybrid renewable energy system. *Int J Precis Eng Manuf Green Technol* 7: 97–117. https://doi.org/10.1007/s40684-019-00101-9
2. Chudy-Laskowska K, Pisula T (2022) An analysis of the use of energy from conventional fossil fuels and green renewable energy in the context of the European Union's planned energy transformation. *Energies* 15: 7369. https://doi.org/10.3390/en15197369

3. Ramirez AD, Rivela B, Boero A, et al. (2019) Lights and shadows of the environmental impacts of fossil-based electricity generation technologies: A contribution based on the Ecuadorian experience. *Energy Policy* 125: 467–477. https://doi.org/10.1016/j.enpol.2018.11.005
4. Kelkar M (2024) Demise of fossil fuels part I: Supply and demand. *Heliyon* 10: e39200. https://doi.org/10.1016/j.heliyon.2024.e39200
5. Covert T, Greenstone M, Knittel CR (2016) Will we ever stop using fossil fuels? *J Econ Perspect* 30: 117–138. https://doi.org/10.1257/jep.30.1.117
6. Van der Ploeg F, Withagen C (2012) Is there really a green paradox? *J Environ Econ Manage* 64: 342–363. https://doi.org/10.1016/j.jeem.2012.08.002
7. Driga AM, Drigas AS (2019) Climate change 101: How everyday activities contribute to the ever-growing issue. *Int J Recent Contrib Eng Sci IT* 7: 22–31. https://doi.org/10.3991/ijes.v7i1.10031
8. Yoro KO, Daramola MO (2020) CO_2 emission sources, greenhouse gases, and the global warming effect. *Adv Carbon Capture*, 3–28. https://doi.org/10.1016/B978-0-12-819657-1.00001-3
9. Singh P, Yadav D (2021) Link between air pollution and global climate change. *Global Clim Change,* 79–108. https://doi.org/10.1016/B978-0-12-822928-6.00009-5
10. Singh RL, Singh PK (2017) Global environmental problems. *Princ Appl Environ Biotechnol Sustainable Future,* 13–41. https://doi.org/10.1007/978-981-10-1866-4_2
11. Richard G, Sawyer WE, Sharipov A (2024) Environmental impacts of air pollution. *Sustainable Strategies for Air Pollut Mitigation,* 47–76. https://doi.org/10.1007/698_2024_1114
12. Algarni S, Tirth V, Alqahtani T, et al. (2023) Contribution of renewable energy sources to the environmental impacts and economic benefits for sustainable development. *Sustainable Energy Technol Assess* 56: 103098. https://doi.org/10.1016/j.seta.2023.103098
13. Kumar S, Rathore K (2023) Renewable energy for sustainable development goal of clean and affordable energy. *Int J Mater Manuf Sustainable Technol* 2: 1–15. https://doi.org/10.56896/IJMMST.2023.2.1.001
14. Cui L, Weng S, Nadeem AM, et al. (2022) Exploring the role of renewable energy, urbanization and structural change for environmental sustainability: Comparative analysis for practical implications. *Renewable Energy* 184: 215–224. https://doi.org/10.1016/j.renene.2021.11.075
15. Neupane D (2022) Biofuels from renewable sources, a potential option for biodiesel production. *Bioengineering* 10: 29. https://doi.org/10.3390/bioengineering10010029
16. Rahpeyma SS, Raheb J (20219) Microalgae biodiesel as a valuable alternative to fossil fuels. *BioEnergy Res* 12: 958–965. https://doi.org/10.1007/s12155-019-10033-6
17. Oni BA, Sanni SE, Orodu DO, et al. (2022) Comparing the effects of Juliflora biodiesel doped with nano-additives on the performance of a compression ignition (CI) engine: Part A. *Energy* 244: 122635. https://doi.org/10.1016/j.energy.2021.122635
18. Mandari V, Devarai SK (2022) Biodiesel production using homogeneous, heterogeneous, and enzyme catalysts via transesterification and esterification reactions: A critical review. *BioEnergy Res* 15: 935–961. https://doi.org/10.1007/s12155-021-10333-w
19. Chidambaram P, Lokhande DA, Ramachandran DM (2021) A review on biodiesel properties and fatty acid composites. *REST J Emerging Trends Modell Manuf* 7: 87–93. https://doi.org/10.46632/7/3/4
20. Aljaafari A, Fattah IMR, Jahirul MI et al. (2022) Biodiesel emissions: a state-of-the-art review on health and environmental impacts. *Energies* 15: 6854. https://doi.org/10.3390/en15186854

21. Litvak S, Litvak O (2020) Some aspects of reducing greenhouse gas emissions by using biofuels. *J Ecol Eng* 21: 198–206. https://doi.org/10.12911/22998993/126967
22. Rony ZI, Mofijur M, Hasan MM, et al. (2023) Alternative fuels to reduce greenhouse gas emissions from marine transport and promote UN sustainable development goals. *Fuel* 338: 127220. https://doi.org/10.1016/j.fuel.2022.127220
23. Thapa S, Indrawan N, Bhoi PR (2018) An overview on fuel properties and prospects of Jatropha biodiesel as fuel for engines. *Environ Technol Innovation* 9: 210–219. https://doi.org/10.1016/j.eti.2017.12.003
24. Sharma AK, Sharma PK, Chintala V, et al. (2020) Environment-friendly biodiesel/diesel blends for improving the exhaust emission and engine performance to reduce the pollutants emitted from transportation fleets. *Int J Environ Res Public Health* 17: 3896. https://doi.org/10.3390/ijerph17113896
25. Ogunkunle O, Ahmed NA (2021) Overview of biodiesel combustion in mitigating the adverse impacts of engine emissions on the sustainable human-environment scenario. *Sustainability* 13: 5465. https://doi.org/10.3390/su13105465
26. Lopresto C (2025) Sustainable biodiesel production from waste cooking oils for energetically independent small communities: an overview. *Int J Environ Sci Technol* 22: 1953–1974. https://doi.org/10.1007/s13762-024-05779-2
27. Mizik T, Gyarmati G (2021) Economic and sustainability of biodiesel production—a systematic literature *review. Clean Technol* 3: 19–36. https://doi.org/10.3390/cleantechnol3010002
28. Naylor RL, Higgins MM (2017) The political economy of biodiesel in an era of low oil prices. *Renewable Sustainable Energy Rev* 77: 695–705. https://doi.org/10.1016/j.rser.2017.04.026
29. Avagyan AB, Singh B (2019) Biodiesel: feedstocks, technologies, economics and barriers. In *Assessment of Environmental Impact in Producing and Using Chains*. https://doi.org/10.1007/978-981-13-5746-6
30. Kumar N, Sonthalia A, Pali HS, et al. (2019) Next-generation biofuels—opportunities and challenges. In *Innovations In Sustainable Energy And Cleaner Environment*, 171–191. https://doi.org/10.1007/978-981-13-9012-8_8
31. Kibar ME, Hilal L, Çapa BT et al. (2023) Assessment of homogeneous and heterogeneous catalysts in transesterification reaction: a mini review. *ChemBioEng Rev* 10: 412–422. https://doi.org/10.1002/cben.202200021
32. Obadiah A, Swaroopa GA, Kumar SV, et al. (2012) Biodiesel production from palm oil using calcined waste animal bone as catalyst. *Bioresour Technol* 116: 512–516. https://doi.org/10.1016/j.biortech.2012.03.112
33. Rizwanul Fattah IM, Ong HC, Mahlia TMI, et al. (2020) State of the art of catalysts for biodiesel production. *Front Energy Res* 8: 101. https://doi.org/10.3389/fenrg.2020.00101
34. de Lima AL, Ronconi CM, Mota CJ (2016) Heterogeneous basic catalysts for biodiesel production. *Catal Sci Technol* 6: 2877–2891. https://doi.org/10.1039/C5CY01989C
35. Miceli M, Frontera P, Macario A, et al. (2021) Recovery/reuse of heterogeneous supported spent catalysts. *Catalysts* 11: 591. https://doi.org/10.3390/catal11050591
36. Abdullah SHYS, Hanapi NHM, Azid A, et al. (2017) A review of biomass-derived heterogeneous catalyst for a sustainable biodiesel production. *Renewable Sustainable Energy Rev* 70: 1040–1051. https://doi.org/10.1016/j.rser.2016.12.008

37. Jayakumar M, Karmegam N, Gundupalli MP, et al. (2021) Heterogeneous base catalysts: Synthesis and application for biodiesel production—A review. *Bioresour Technol* 331: 125054. https://doi.org/10.1016/j.biortech.2021.125054
38. Orege JI, Oderinde O, Kifle GA, et al. (2022) Recent advances in heterogeneous catalysis for green biodiesel production by transesterification. *Energy Convers Manage* 258: 115406. https://doi.org/10.1016/j.enconman.2022.115406
39. Bhuiya M, Rasul M, Khan M, et al. (2016) Prospects of 2nd generation biodiesel as a sustainable fuel—Part: 1 selection of feedstocks, oil extraction techniques and conversion technologies. *Renewable Sustainable Energy Rev* 55: 1109–1128. https://doi.org/10.1016/j.rser.2015.04.163
40. Gaurav N, Sivasankari S, Kiran G, et al. (2017) Utilization of bioresources for sustainable biofuels: A review. *Renewable Sustainable Energy Rev* 77: 205–214. https://doi.org/10.1016/j.rser.2017.01.070
41. Bindra S, Sharma R, Khan A, et al. (2017) Renewable energy sources in different generations of bio-fuels with special emphasis on microalgae derived biodiesel as sustainable industrial fuel model. *Biosci Biotechnol Res Asia* 14: 259–274. https://doi.org/10.13005/bbra/2443
42. Hamza M, Ayoub M, Shamsuddin R, et al. (2021) A review on the waste biomass derived catalysts for biodiesel production. *Environ Technol Innovation* 21: 101200. https://doi.org/10.1016/j.eti.2020.101200
43. Hussain F, Alshahrani S, Abbas MM, et al. (2021) Waste animal bones as catalysts for biodiesel production: A mini review. *Catalysts* 11: 630. https://doi.org/10.3390/catal11050630
44. Yang LM, Lv PM, Yuan ZH, et al. (2012) Synthesis of biodiesel by different carriers supported KOH catalyst. *Adv Mater Res* 581: 197–201. https://doi.org/10.4028/www.scientific.net/AMR.581-582.197
45. Okechukwu OD, Joseph E, Nonso UC, et al. (2022) Improving heterogeneous catalysis for biodiesel production process. *Cleaner Chem Eng* 3: 100038. https://doi.org/10.1016/j.clce.2022.100038
46. Ferreira RSB, dos Passos RM, Sampaio KA, et al. (2019) Heterogeneous catalysts for biodiesel production: A review. *Food Public Health* 9: 125–137. https://doi.org/10.5923/j.fph.20190904.04
47. Efeovbokhan VE, Omoleye JA, Kalu EE, et al. (2017) Kinetics of base catalysed trans-esterification of jatropha oil using potassium hydroxide extract from ripe plantain peels. *Int J Appl Eng Res* 12: 4539–4548. Available from: https://www.ripublication.com/ijaer17/ijaerv12n14_62.pdf.
48. Hsiao MC, Liao PH, Lan NV, et al. (2021) Enhancement of biodiesel production from high-acid-value waste cooking oil via a microwave reactor using a homogeneous alkaline catalyst. *Energies* 14: 437. https://doi.org/10.3390/en14020437
49. Awogbemi O, Onuh EI, Inambao FL (2019) Comparative study of properties and fatty acid composition of some neat vegetable oils and waste cooking oils. *Int J Low-Carbon Technol* 14: 417–425. https://doi.org/10.1093/ijlct/ctz038
50. Chanakaewsomboon I, Phoungthong K, Palamanit A, et al. (2023) Biodiesel produced using potassium methoxide homogeneous alkaline catalyst: Effects of various factors on soap formation. *Biomass Convers Biorefin* 13: 9237–9247. https://doi.org/10.1007/s13399-021-01787-1
51. Hsiao MC, Lin WT, Chiu WC, et al. (2021) Two-Stage biodiesel synthesis from used cooking oil with a high acid value via an ultrasound-assisted method. *Energies* 14: 3703. https://doi.org/10.3390/en14123703

52. Ayodeji A, Gozirim C, Cedar A, et al. (2023) Production of waste vegetable oil biodiesel using calcined periwinkle shells as catalyst. *Chem Pap* 77: 6647–6654. https://doi.org/10.1007/s11696-023-02965-3
53. Roslan NA, Abidin SZ, Abdullah NO, et al. (2022) Esterification reaction of free fatty acid in used cooking oil using sulfonated hypercrosslinked exchange resin as catalyst. *Chem Eng Res Des* 180: 414–424. https://doi.org/10.1016/j.cherd.2021.10.020
54. Chowdhury A, Sarkar D, Mitra D (2016) Esterification of free fatty acids derived from waste cooking oil with octanol: Process optimization and kinetic modeling. *Chem Eng Technol* 39: 730–740. https://doi.org/10.1002/ceat.201400745
55. Oo YM, Prateepchaikul G, Somnuk K (2021) Two-stage continuous production process for fatty acid methyl ester from high FFA crude palm oil using rotor-stator hydrocavitation. *Ultrason Sonochem* 73: 105529. https://doi.org/10.1016/j.ultsonch.2021.105529
56. Tovar AM, Valencia LF, Villa AL (2024) Life cycle assessment of Colombian cocoa pod husk transformation into value-added products. *Bioresour Technol Rep* 2024: 101772. https://doi.org/10.1016/j.biteb.2024.101772
57. Xue S, Li M, Jiang J, et al. (2019) Phosphogypsum stabilization of bauxite residue: conversion of its alkaline characteristics. *J Environ Sci* 77: 1–10. https://doi.org/10.1016/j.jes.2018.05.016
58. Özgür C (2021) Optimization of biodiesel yield and diesel engine performance from waste cooking oil by response surface method (RSM.). *Pet Sci Technol* 39: 683–703. https://doi.org/10.1080/10916466.2021.1954019
59. Tavizón-Pozos JA, Chavez-Esquivel G, Suárez-Toriello VA, et al. (2021) State of art of alkaline earth metal oxides catalysts used in the transesterification of oils for biodiesel production. *Energies* 14: 1031. https://doi.org/10.3390/en14041031
60. Maroa S, Inambao F (2021) A review of sustainable biodiesel production using biomass derived heterogeneous catalysts. *Eng Life Sci* 21: 790–824. https://doi.org/10.1002/elsc.202100025
61. Lee HV, Juan JC, Yun Hin TY, et al. (2016) Environment-friendly heterogeneous alkaline-based mixed metal oxide catalysts for biodiesel production. *Energies* 9: 611. https://doi.org/10.3390/en9080611
62. Ofori P (2017) Production of potassium hydroxide (KOH) from plant biomass: The case of cocoa pod husks and plantain peels. Master's thesis, Kwame Nkrumah University of Science and Technology, Kumasi. Available from: PRODUCTION-OF-POTASSIUM-HYDROXIDE-KOH-FROM-PLANT-BIOMASS-THE-CASE-OF-COCOA-POD-HUSKS-AND-PLANTAIN-PEELS.pdf.
63. Xie W, Li J (2023) Magnetic solid catalysts for sustainable and cleaner biodiesel production: A comprehensive review. *Renewable Sustainable Energy Rev* 171: 113017. https://doi.org/10.1016/j.rser.2022.113017
64. Qu T, Niu S, Zhang X, et al. (2021) Preparation of calcium modified Zn-Ce/Al_2O_3 heterogeneous catalyst for biodiesel production through transesterification of palm oil with methanol optimized by response surface methodology. *Fuel* 284: 118986. https://doi.org/10.1016/j.fuel.2020.118986
65. Gülüm M, Yesilyurt MK, Bilgin A (2020) The modeling and analysis of transesterification reaction conditions in the selection of optimal biodiesel yield and viscosity. *Environ Sci Pollut Res* 27: 10351–10366. https://doi.org/10.1007/s11356-019-07473-0

66. Hassan MM, Fadhil AB (2025) Development of an effective solid base catalyst from potassium based chicken bone (K-CBs) composite for biodiesel production from a mixture of non-edible feedstocks. *Energy Sources, Part A* 47: 8056–8071. https://doi.org/10.1080/15567036.2021.1927253
67. Yadav M, Singh V, Sharma YC (2017) Methyl transesterification of waste cooking oil using a laboratory synthesized reusable heterogeneous base catalyst: Process optimization and homogeneity study of catalyst. *Energy Convers Manage* 148: 1438–1452. https://doi.org/10.1016/j.enconman.2017.06.024
68. Dong Z, Dong K, Li H, et al. (2025) Progress and challenges in the process of using solid waste as a catalyst for biodiesel synthesis. *Molecules* 30: 3243. https://doi.org/10.3390/molecules30153243
69. Faruque MO, Razzak SA, Hossain MM (2020) Application of heterogeneous catalysts for biodiesel production from microalgal oil—A review. *Catalysts* 10: 1025. https://doi.org/10.3390/catal10091025
70. Ismail S, Ahmed AS, Anr R, et al. (2016) Biodiesel production from castor oil by using calcium oxide derived from mud clam shell. *J Renewable Energy*. https://doi.org/10.1155/2016/5274917
71. Miyuranga KV, Arachchige US, Marso T (2023) Biodiesel production through the transesterification of waste cooking oil over typical heterogeneous base or acid catalysts. *Catalysts* 13: 546. https://doi.org/10.3390/catal13030546
72. Ajala E, Ajala M, Okedere O, et al. (2021) Synthesis of solid catalyst from natural calcite for biodiesel production: Case study of palm kernel oil in an optimization study using definitive screening design. *Biofuels* 12: 703–714. https://doi.org/10.1080/17597269.2018.1532752
73. Animasaun DA, Ameen MO, Belewu MA (2021) Protocol for biodiesel production by base-catalyzed transesterification method. In *Biofuels and Biodiesel*, 103–113. https://doi.org/10.1007/978-1-0716-1323-8_7
74. Kalsoom M, El Zerey-Belaskri A, Nadeem F, et al. (2017) Fatty acid chain length optimization for biodiesel production using different chemical and biochemical approaches—a comprehensive review. *Int J Chem Biochem Sci* 11: 75–94. Available from: https://www.iscientific.org/wp-content/uploads/2020/05/10-IJCBS-17-11-10.pdf.
75. Maina L, Rabiu A, Ojumu T, et al. (2023) An investigation of the potential of a bifunctional catalyst in biodiesel production from low-cost feedstocks. *Waste Biomass Valorization* 14: 805–821. https://doi.org/10.1007/s12649-022-01862-2
76. Maheshwari AS, Chellani JG (2012) Correlations for pour point and cloud point of middle and heavy distillates using density and distillation temperatures. *Fuel* 98: 55–60. https://doi.org/10.1016/j.fuel.2012.02.034
77. Kumar S, Shamsuddin MR, Farabi MA, et al. (2020) Production of methyl esters from waste cooking oil and chicken fat oil via simultaneous esterification and transesterification using acid catalyst. *Energy Convers Manage* 226: 113366. https://doi.org/10.1016/j.enconman.2020.113366
78. Nisa S, Hanif MA, Rashid U, et al. (2021) Trends in widely used catalysts for fatty acid methyl esters (Fame) production: A review. *Catalysts* 11: 1085. https://doi.org/10.3390/catal11091085
79. Rashid IM, Atiya MA, Hameed B (2015) Production of biodiesel from waste cooking oil using CaO-egg shell waste derived heterogeneous catalyst. *Int J Sci Res* 6: 94–103. https://doi.org/10.21275/ART20177723

80. Haq IU, Akram A, Nawaz A (2021) Comparative analysis of various waste cooking oils for esterification and transesterification processes to produce biodiesel. *Green Chem Lett Rev* 14: 462–473. https://doi.org/10.1080/17518253.2021.1941305
81. Kedir WM, Wondimu KT, Weldegrum GS (2023) Optimization and characterization of biodiesel from waste cooking oil using modified CaO catalyst derived from snail shell. *Heliyon* 9: e16475. https://doi.org/10.1016/j.heliyon.2023.e16475
82. Li G, Hou B, Wang A, et al. (2019) Making JP-10 superfuel affordable with a lignocellulosic platform compound. *Angew Chem Int Ed* 58: 12154–12158. https://doi.org/10.1002/anie.201906744
83. Kim D, Martz J, Abdul-Nour A (2017) A six-component surrogate for emulating the physical and chemical characteristics of conventional and alternative jet fuels and their blends. *Combust Flame* 179: 86–94. https://doi.org/10.1016/j.combustflame.2017.01.025

AIMS Press